J. Entomol. Res. Soc., 27(3): 429-444, 2025 *Research Article*
Doi: 10.51963/jers.v27i3.2883 *Online ISSN:2651-3579*

Cloning and Expression Characteristics of Sorbitol Dehydrogenase Gene *EiSD* under Temperature Stress in *Epicauta impressicornis*

Qing YANG[1, 2, 3a] Yangyang LIU[4b] Xiangsheng CHEN[1, 2, 3c*]

[1]Guizhou Key Laboratory of Agricultural Biosecurity, Guizhou University, Guiyang 550025, CHINA

[2]Institute of Entomology, Guizhou University, Guiyang 550025, CHINA

[3]The Provincial Special Key Laboratory for Development and Utilization of Insect Resources, Guizhou University, Guiyang 550025, CHINA

[4]Guizhou Key Laboratory of Agricultural Biosecurity, Guiyang University, Guiyang, 550005, CHINA

e-mails: [a]yqing112511@163.com; [b]tadouliuyy@126.com; [c]chenxs3218@163.com

ORCID IDs: [a]0009-0003-0389-9808; [b]0000-0003-2502-5194; [c]0000-0001-8750-8410

*Corresponding Author

ABSTRACT

Epicauta impressicornis Pic. (Coleoptera: Meloidae), an insect of profound medicinal significance, synthesizes cantharidin, a compound known for its anticancer effects. To investigate the expression characteristics of the *EiSD* gene in *E. impressicornis* and its temperature adaptability. In this study, we cloned *E. impressicornis'* sorbitol dehydrogenase gene (*EiSD*) (GenBank accession number: PV394100), and analyzed its bioinformatic characterization, and profiled its expression across developmental stages, tissues, and under various temperatures stress conditions. *EiSD* has a 1,071 bp ORF that encodes 356 amino acids, with a molecular weight of 38.90 kDa, an isoelectric point of 6.42, and a half-life of 30 h. Phylogenetic analysis showed that it is highly conserved and closely related to the SD of *Tribolium castaneum* (Herbst). Real-time quantitative PCR (RT-qPCR) revealed that *EiSD* expression peaks in the thorax, and is lowest in the 5th instar larvae and at 12, 18, and 36 °C. The results suggest that *EiSD* is essential for withstanding low and extreme temperatures. Its low expression under extreme temperature stress likely modulates the sorbitol metabolic pathway, leading to cryoprotectant sorbitol accumulation that supports larval diapaused and stress resistance.

Keywords: Medicinal insect, *Epicauta impressicornis*, *EiSD* gene, RT-qPCR analysis, temperature adaptation, expression patterns.

Yang, Q., Liu, Y., & Chen, X. (2025). Cloning and expression characteristics of sorbitol dehydrogenase gene *EiSD* under temperature stress in *Epicauta impressicornis*. *Journal of the Entomological Research Society*, 27(3), 429-444.

Received: April 23, 2025 *Accepted: November 26, 2025*

INTRODUCTION

Meloid beetles (family Meloidae) are of significant medicinal value due to their cantharidin content, serving as a traditional Chinese medicinal resource (Jakovac-Strajn et al., 2021). In recent years, the demand for cantharidin has increased, driven by its extensive clinical applications in the treatment of skin diseases, liver cancer, rabies, and various other types of cancers (Coloe & Morrell, 2009; Zou, Xu, Lin, Zhou, & Xia, 2023; Yang et al., 2023; Tang et al., 2024; Duan et al., 2025). Nevertheless, the principal source of medicinal cantharidin and its derivatives continues to be wild meloid beetles. The limited availability of these beetles poses a challenge for achieving a sustainable supply (Deng et al., 2017). Moreover, the artificial synthesis of cantharidin encounters obstacles due to stringent reaction conditions and high production costs. Consequently, the large-scale artificial rearing of meloid beetles is viewed as a practical solution to mitigate the scarcity of cantharidin resources. However, the unique life-history traits of Meloidae beetles, including their intricate metamorphosis and prolonged diapause phases (Chen & Tu, 2013), present considerable constraints on artificial rearing efforts and the exploitation of these resources.

Sorbitol dehydrogenase holds a pivotal role in insect metabolic physiology. It serves as a key enzyme in sorbitol metabolism, not only catalyzing the oxidation of sorbitol to fructose and directing it into the fructose metabolic pathway (Milagre & Milagre, 2022), but also participating in the conversion of sorbitol to glucose through the glucitol reductase pathway, thereby significantly impacting insect development. In the face of adverse environmental conditions, such as low temperatures, insects adopt diapause as an adaptive survival strategy. During this state, they accumulate substantial sorbitol reserves to improve cold tolerance (Xie et al., 2023). Insects like *Aphidoletes aphidimyza* (Rondani), *Bactrocera minax* (Enderlein), and *Bemisia argentifolii* (Bellows and Perring) rely heavily on sorbitol as their energy source during diapause, with sorbitol dehydrogenase being indispensable for this metabolic process (Dai et al., 2024). As environmental temperatures increase, insects transition from diapause to active developmental stages, experiencing a surge in energy demands. At this critical juncture, sorbitol dehydrogenase activity spikes to metabolize the accumulated sorbitol into glucose, providing essential energy for insect growth and development - a phenomenon clearly observed in *Drosophila melanogaster* (Meigen) (Marks, 2020). Furthermore, diapause is not only an evolutionary strategy for insects to cope with harsh environments, but also involves a series of physiological and biochemical adaptations (Mohammadzadeh, Borzoui, & Izadi, 2017). These adaptive changes bolster insect resilience to environmental stressors and profoundly affect their reproduction, survival, and evolutionary paths (Wang & Li, 2004; Jiang et al., 2021). For example, diapausing larvae of the wheat midge *Sitodiplosis mosellana* (Géhin) exhibit significant sorbitol accumulation, which enhances their cold tolerance (Liu, Li, Yang, Chi, & Chen, 2018). Thus, sorbitol dehydrogenase is essential in the transition from diapause to normal development in insects, acting as a key factor in their adaptation to temperature fluctuations and ensuring adequate growth and development. Despite the current understanding of the critical role of sorbitol dehydrogenase genes in

temperature stress resistance across various insect species, no reports exist on the temperature-stress response of the *SD* gene in *E. impressicornis*.

Building upon our previous transcriptomic research on *E. impressicornis*, the present study delves into the response of the sorbitol dehydrogenase gene under temperature stress conditions. Utilizing qPCR technology and bioinformatics methodologies, we cloned and characterized the *EiSD* gene. Its amino-acid sequence was aligned with SD proteins from six Coleopteran species and then integrated with SD sequences from 17 insects across four orders (Lepidoptera, Coleoptera, Hymenoptera, and Diptera) to reconstruct the phylogenetic tree. Additionally, we employed RT-qPCR to investigate its expression profiles across various developmental stages, different tissues and under various temperature stress conditions of 5th instar larvae. The objective of this study is to establish a theoretical framework for understanding the functional role of the *EiSD* gene in *E. impressicornis* and its temperature-adaptive mechanisms. Moreover, it provides a scientific basis for the sustainable artificial rearing of Meloidae beetles.

MATERIALS AND METHODS

Test Insect Sources and Treatments

The test insects employed in this study were collected in September 2023 from the Huaxi District of Guiyang City, Guizhou Province (106.88°E, 26.57°N). *E.impressicornis* was reared in an artificial climate chamber under strictly controlled conditions (temperature: 30 °C, humidity: 75% ± 5%, photoperiod: L_{14}:D_{10}). The larvae were fed grasshopper eggs, the pupal stage was non-feeding, and the adults were provided with pumpkin (Liu, Li, Yang, Chi, & Chen, 2018; Liu, Zhou, & Chen, 2020; Liu, Zhou, & Chen, 2024).

Given that 5th instar larvae entered diapause for overwintering, this study utilized 4th instar larvae (L4) at 24 h, 48 h, and 72 h, 5th instar larvae (L5), and pupae (P) at different developmental stages. To perform tissue isolation, three healthy 5th instar larvae were anesthetized by chilling. Under sterile conditions, dissection was carried out using disinfected scalpels and forceps. Specifically, the head was separated at the head-thorax junction, the thoracic tissue was excised from the anterior forehead region, and the abdominal segments were obtained through a dorsal incision. The reticulate fat body was carefully removed, and the Malpighian tubules were isolated at the junction between the midgut and hindgut. All tissues were immediately placed in pre-chilled RNAlater, washed to remove the preservative via centrifugation, and stored at -80°C for subsequent use. The 5th instar larvae of *E. Impressicornis* were exposed to temperature treatments within artificial climate chambers set at 12, 18, 24, 30, and 36 °C(relative humidity: 75%±5%, photoperiod: L_{14}:D_{10}) for 24 h (Liu, Li, Yang, Chi, & Chen, 2018; Liu, Zhou, & Chen, 2024). For each treatment group, three insects were combined to form one biological sample, with three replicates conducted per group. All samples were subsequently stored at -80 °C for further analysis. All experimental treatments and gene cloning procedures were carried out between June 2023 and June 2024 in Laboratories C401-C404 of the Guizhou Key Laboratory for Agricultural Biosafety, Guiyang University.

Total RNA Extraction and cDNA Synthesis

RNA extraction was carried out in accordance with the protocol provided by the manufacturer for the HP Total RNA Kit (R6812-01). The quality of the extracted total RNA was assessed using a suite of methods, including 1% agarose gel electrophoresis, a Nanodrop spectrophotometer, and the Agilent 2100 Bioanalyzer. These assessments were conducted to ensure the absence of contamination, the purity, and the integrity of the RNA samples. The extracted total RNA was then diluted to a concentration of approximately 1000 ng/μL with DEPC-treated water, followed by the synthesis of cDNA as per the instructions provided with the PrimeScript® RT reagent Kit, which included the gDNA Eraser.

Cloning of the *EiSD*

The gene sequence alignment was performed using known homologous insect *SD* sequences and the *E. impressicornis* transcriptome data (GenBank accession number: PRJNA679947) to identify conserved regions. Primers for the amplification of the *SD* gene in *E. impressicornis* were designed using Primer Premier 5.0 software (Table 1). The cDNA, which was synthesized using diapausing 5th instar larvae of *E. impressicornis* as the template, was utilized as the template for amplifying the *SD* gene. The 25 μL PCR reaction mixture was composed of the 1 μL of cDNA template, 1 μL of each forward and reverse primers (*EiSD*-F/R), 12.5 μL of Taq Mix, and 9.5 μL of ddH_2O. The amplification protocol included an initial denaturation step at 95 °C for 5 minutes, followed by 33 cycles of denaturation at 95 °C for 30 s, annealing at 55 °C for 30 s, and extension at 72 °C for 2 mins. This was concluded with a final extension at 72 °C for 10 mins, after which the reaction was held at 4 °C. The target DNA fragments were subsequently gel-extracted and purified using Magen's HiPure Gel Pure DNA Mini Kit, adhered strictly to the manufacturer's instructions. The purified PCR products were then ligated into the PMD18-T vector and transformed into DH5α competent cells. Positive clones were screened and sent to SunYa Biotech for DNA sequencing.

Table 1. Information on primers related to the *EiSD*.

Primers	Primer sequences (5' - 3')	Purpose
EiSD-F	CGTATTTTAGCACTGCAACAA	Full-length sequence amplification
EiSD-R	ATCTGCAGCTTTTCTATTACGT	
q*EiSD*-F	GCTATCAAGTGCCTGGTATC	Target gene amplification in real-time quantitative PCR
q*EiSD*-R	GAGATGAGATGTGGAAACGAAA	
q*GAPDH*-F	TTGGTTCTGTGCGATGTG	Reference gene amplification in real-time quantitative PCR
q*GAPDH*-R	TGTTCCTCGTCCAGTATCA	

The Bioinformatics Analysis of *EiSD*

Homology analysis was performed using the BLAST available through the NCBI (https://blast.ncbi.nlm.nih.gov/Blast.cgi). The open reading frame (ORF) and the corresponding amino acid sequence were predicted using ORF Finder (https://www.ncbi.nlm.nih.gov/orffinder/). The molecular weight and isoelectric point of the encoded protein were determined using the online Protparam tool (https://web.expasy.org/protparam/). N-glycosylation sites were predicted using the NetNGlyc1.0 Server (http://www.cbs.dtu.dk/services/NetNGlyc/), while phosphorylation sites were predicted with

Kinaseihos (http://kinaseihos.mbc.nctu.edu.tw/). The presence of a signal peptide was predicted using SignalP4.1 Server (http://www.cbs.dtu.dk/services/SignalP/), and transmembrane domains were identified with the TMHMM v.2.0 program (http://www.cbs.dtu.dk/services/TMHMM/). Analysis of conserved motifs in the SD amino acid sequences of the *E. impressicornis* and six other insects (Coleoptera: *Sitophilus oryzae* (Linnaeus), *Dendroctonus ponderosae* (Hopkins), *Onthophagus taurus* (Schreber), *Photinus pyralis* (Linnaeus), *Leptinotarsa decemlineata* (Say), *Tribolium castaneum* (Herbst) was performed using DNAMAN7.0 software and ScanProsite (https://prosite.expasy.org/scanprosite/). The cloned gene was subjected to homology modeling using SWISS-MODEL (http://www.swissmodel.expasy.org/interactive/), and its tertiary protein structure was visualized with PyMOL. Cluster analysis of amino acid sequences was performed using MEGA-X. Homologous SD amino acid sequences from four orders - Lepidoptera, Coleoptera, Hymenoptera, and Diptera—were obtained from 17 species. A Neighbor-Joining (NJ) phylogenetic tree was constructed using MEGA-X with the p-distance and 1000 bootstrap replications to assess nodal support.

RT-qPCR Analysis of *EiSD*

RT-qPCR was employed to quantify the expression levels of *EiSD* across various developmental stages, in different tissues of the 5th instar larvae, and under different temperature treatments, using glyceraldehyde-3-phosphate dehydrogenase (*GAPDH*) as the endogenous reference gene (Table 1). Primers specific for *EiSD* and the reference gene were designed and used following the guidelines provided in the TB Green® Premix DimerEraser™ kit manual (TaKaRa). The reaction mixture was prepared as follows: 1 μL of cDNA template, 10 μL of TB Green Premix Ex Taq, 0.4 μL of ROX Reference Dye II, 1 μL each of forward and reverse primers, and 6.6 μL of ddH_2O to make up a total reaction volume of 20 μL. The thermal cycling protocol included an initial denaturation step *denaturation* at 95 °C for 5 min, followed by 40 cycles of *denaturation* 95 °C for 5 s and extension at 57 °C for 40 s.

Data Analysis

The relative expression of *EiSD* was calculated using the $2^{-\Delta\Delta Ct}$ method (Livak & Schmittgen, 2001). Differences in *EiSD* relative expression levels across developmental stages, tissues types, and temperature treatments were analyzed using IBM SPSS Statistics 22 software (Landau & Everitt, 2004), employing one-way ANOVA, followed by Tukey's post hoc test with a significance level established at $p<0.05$. Expression data were visualized using Excel 2025.

RESULTS

Cloning and Sequence Analysis of *EiSD*

The *EiSD* sequence was successfully obtained via amplification cloning and assigned the GenBank accession number PV394100. The full-length cDNA sequence of the *EiSD* gene was 1,253bp, encompassing an open reading frame (ORF) of

1,071 bp that encodes 356 amino acids (Fig. 1). The 5' untranslated region (UTR) consisted of 34 bp, while the 3' UTR was composed of 179 bp. The deduced amino acid sequence had the molecular formula $C_{1725}H_{2785}N_{473}O_{505}S_{21}$, commencing with the N-terminal methionine (Met). The theoretical molecular weight, isoelectric point, and half-life were calculated to be 38.90 kDa, 6.42, and 30 hours, respectively. Further analysis of the EiSD revealed that it contained 20 amino acids types, with valine (Val) being the most prevalent at 11.5%, followed by glycine (Gly) at 8.4%, and isoleucine (Ile) at 8.1%. The protein contained a total of 42 negatively charged residues (aspartic acid, Asp + glutamic acid, Glu) and 39 positively charged residues (arginine, Arg + lysine, Lys). The instability index was 28.72 (<40), the lipophilicity index was 100.11, and the corresponding average hydrophobicity was -0.003 (Table 2). The *EiSD* protein possessed three potential glycosylation sites at positions N_6, N_{125}, and N_{243}, and four phosphorylation sites, which included three serine phosphorylation sites (S_{145}, S_{156} and S_{249}) and one threonine phosphorylation site (T_{72}). The protein featured a single transmembrane structure, highlighted in gray, and lacked a signal peptide (Fig. 1 and Table 2).

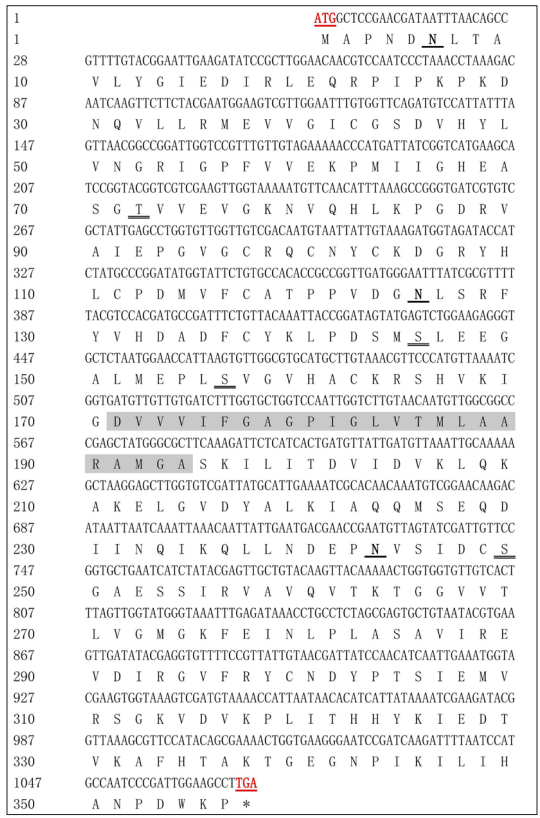

Figure 1. Nucleotide and deduced amino acid sequences of *EiSD.*

A red single underline and an asterisk reiresents the start codon (ATG) and the termination codon (TAG,a bold single underline is the glycosylation sites, the double underline is the phosphorylation sites, the shaded part is the transmembrane helix regions.

Table 2. Physical and chemical properties of EiSD.

Item	*EiSD*
Protein molecular formula	$C_{1725}H_{2785}N_{473}O_{505}S_{21}$
Relative molecular mass (kDa)	38.9
Theoretical isoelectric point (pI)	6.42
Ala content (%)	6.5
Arg content (%)	4.2
Asn content (%)	3.9
Asp content (%)	6.5
Cys content (%)	2.8
Gln content (%)	3.1
Glu content (%)	5.3
Gly content (%)	8.4
His content (%)	3.1
Ile content (%)	8.1
Leu content (%)	7.3
Lys content (%)	6.7
Met content (%)	3.1
Phe content (%)	2.2
Pro content (%)	5.9
Ser content (%)	4.5
Thr content (%)	3.7
Trp content (%)	0.3
Tyr content (%)	2.8
Val content (%)	11.5
Total number of negatively charged residues	42
Total number of positively charged residues	39
Extinction coefficient	21025
Half-life (h)	30
Instability coefficient	28.72
Fat coefficient	100.11
Average hydropathicity coefficient	-0.003

The hydrophobicity scores of the EiSD exhibited considerable variation across the sequence, suggesting the presence of both hydrophobic and hydrophilic regions within the structure. Specifically, the hydrophobicity values were notably positive between amino acid positions 50 to 150, 250 to 350, and 450 to 550. In contrast, the values were negative between positions approximately 150 to 250 and 350 to 450. The most hydrophobic segment possessed a score of 2.3, whereas the least hydrophobic region had a value of -2.178, indicating that the EiSD was predominantly hydrophilic (Fig. 2). The protein was predicted to contain a single transmembrane structure, which categorized it as a transmembrane protein (Fig. 3). Phosphorylation-site prediction for the EiSD revealed varying phosphorylation potential of serine, threonine, and tyrosine across the protein sequence. Serine phosphorylation potential surpassed the set threshold at numerous positions. Threonine and tyrosine also exceeded the threshold, but less frequently than serine (Fig. 4). The cellular localization of the *EiSD* indicated that it was predominantly situated in the mitochondria, accounting for 34.80% of its distribution, followed by the cytoplasm at 30.40%, the Golgi apparatus at 13.00%, and the endoplasmic reticulum at 8.90%. Additionally, the protein was found in the

nucleus, extracellularly (including the cell wall), and within secretory system vesicles, each representing 4.30% of its distribution (Fig. 5).

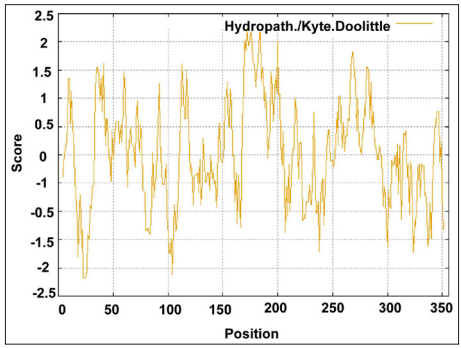

Figure 2. Visualization of the hydrophobicity of the EiSD protein amino acids. Score > 0, hydrophobicity; Score < 0, hydrophilic.

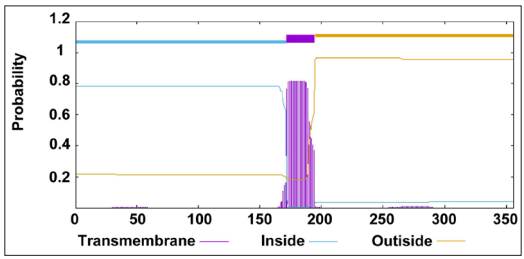

Figure 3. Transmembrane structure prediction results for EiSD proteins.

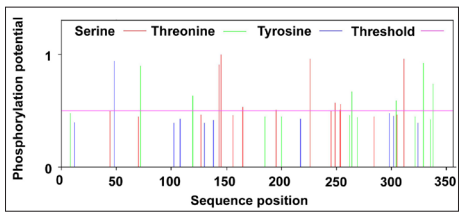

Figure 4. Prediction of phosphorylation sites of EiSD.

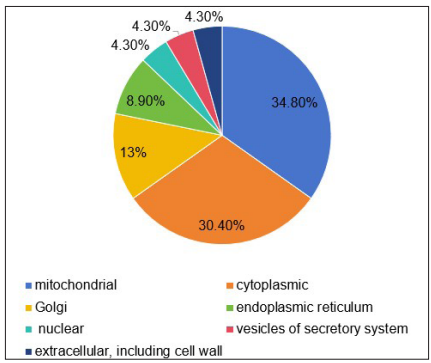

Figure 5. Proportion of EiSD protein at different positions.

Protein Structure Analysis of EiSD

The secondary structure of the EiSD was predicted using the online software SOPMA, which revealed that the protein was largely composed of random coils, accounting for 62.64% of the total amino acid chain. Moreover, α-helices contributed 12.64%, while extended strands comprised 24.72% of the structure (Fig. 6). The tertiary structure of the EiSD protein was modeled using SWISS-MODEL. For 3D modeling was *Curculio ferrugineu*s (Olivier) (SMTL ID: A0A834IPY3.1.A) served as the reference protein, and the predicted global model quality was estimated at 0.97, indicating a high degree of reliability in the structure prediction (>0.8). The sequence identity between the EiSD and the reference protein was 71.07% (Fig. 7).

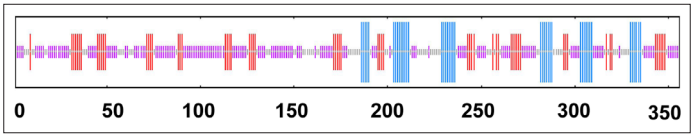

Figure 6. Prediction of secondary structure of EiSD proteins. Purple line: random coil; Red line: extension chain; Blue line: α-helix.

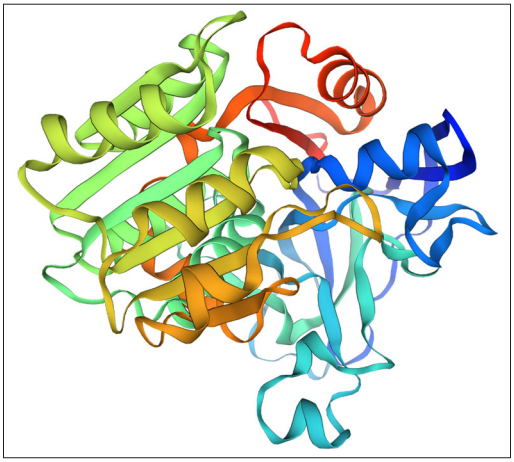

Figure 7. Prediction of the tertiary structure of ***EiSD*** proteins.

Comparative homology and phylogenetic analysis of EiSD

The amino acid sequence of EiSD from *E. impressicornis* was compared with SD sequences from *S. oryzae*, *D. ponderosae*, *O. taurus*, *P. pyralis*, *L. decemlineata*, and *T. castaneum*. These SD homologs share 78.02% sequence identity, reflecting a high degree of conservation. Insect SDs contain several conserved motifs, notably DRLTAVLY, RLEQRP, VGICGSDVHY and IGHEA (Fig. 8). The NCBI database was searched for EiSD amino acid sequences from 17 additional insects, encompassing 7 from the Coleoptera, 3 from Diptera, 2 from Hymenoptera, and 2 from the outgroup Hemiptera. A neighbour-joining (NJ) phylogenetic tree was constructed from the EiSD amino acid sequences (Fig. 9). The phylogenetic analysis revealed that Coleoptera,

Diptera, Hymenoptera, and Hemiptera constituted a separate cluster, indicating a significant level of conservation of the EiSD protein across these insect groups. Within the Coleoptera order, *E. impressicornis* exhibited the closest evolutionary relationship with *T. castaneum*. Both species were clustered together with *S. oryzae*, *D. ponderosae*, and *L. decemlineata*, forming a well-supported clade. This group was most distantly related to the outgroup Hemiptera, which was consistent with the established insect taxonomic classifications.

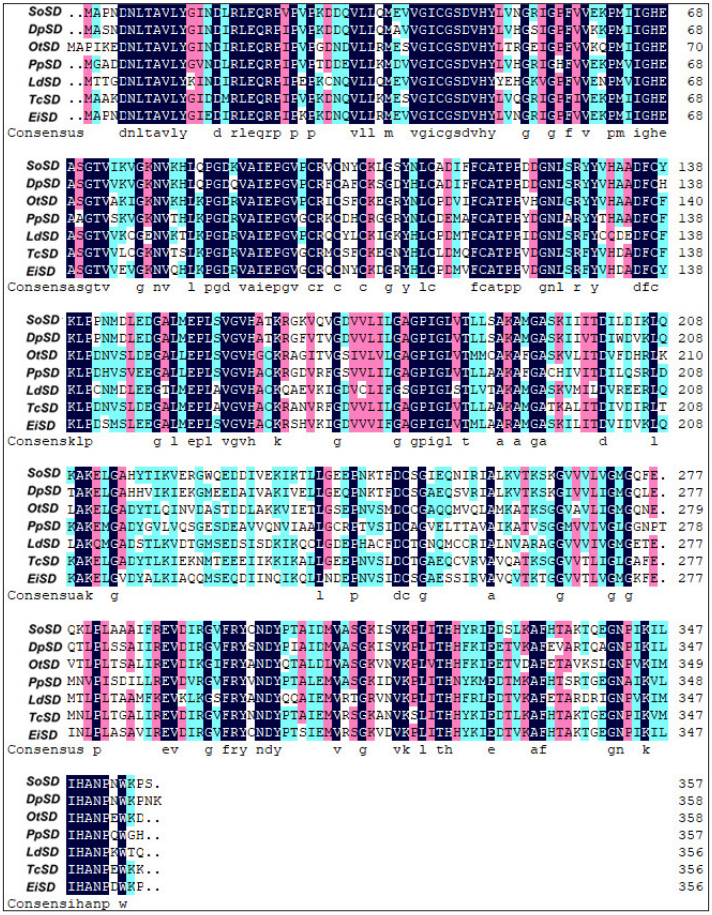

Figure 8. Comparison of the amino acid sequence of the *E. impressicornis* SD protein with the sequences of other species. Note: The black blue base similarity is 100%; the purple red background base similarity is 100% to 75%; and the light blue background base similarity is 75% to 50%. The sequence information were from NCBI (SoSD: *S. oryzae* XP_030754708.1, DpSD: *D. ponderosae* XP_019755864.1, OtSD: *O. taurus* XP_022913174.1, PpSD: *P. pyralis* XP_031330097.1, LdSD: *L. decemlineata* XP_023016450.1, TcSD: *T. castaneum* XP_972368.1).

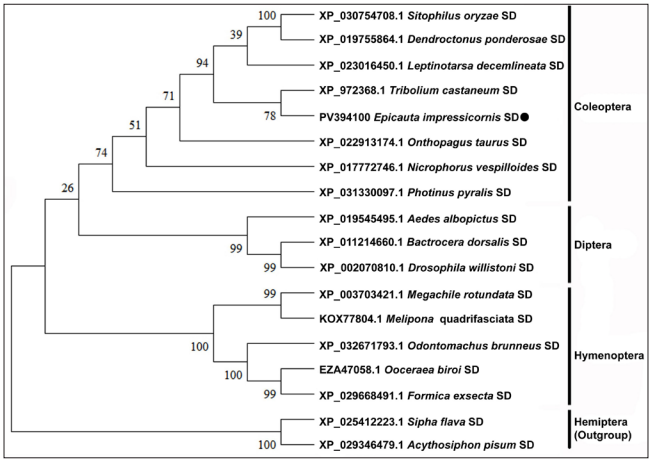

Figure 9. Phylogenetic analysis of insect *EiSD* based on amino acid sequence.

(The values at the branch points represent the confidence of bootstrap values calculated from 1000 clustering iterations, with the point labeled as the *EiSD*).

Expression Analysis of *EiSD*

The relative expression levels of *EiSD* exhibited variation across developmental stages of *E. impressicornis*. We examined 4th instar larvae, 5th instar larvae, and pupae, with samples collected at 24 h (L4-1, L5-1, P1), 48 h (L4-2, L5-2, P2), and 72 h (L4-3, L5-3, P3). The expression pattern of *EiSD* showed an initial decrease followed by a partial increase (Fig. 10). The expression level in the 5th instar larvae was significantly lower compared with in 4th instar larvae and pupal stage (L_5 vs. L_4/P: $p < 0.05$). The expression of *EiSD* was lowest at 72 h in 5th instar larvae, highest at 24 h in 4th instar larvae, and second highest at 72 h in pupal stage. There was a significant decline in *EiSD* expression from 4th to the 5th instar larvae (L_4 vs. L_5: $p < 0.05$), which then started to rise upon pupation before gradually decreasing (Fig. 10).

The relative expression levels of the *EiSD* gene differed across various tissues in the 5th instar larvae of *E. impressicornis*. The thoracic region exhibited significantly higher expression levels compared to other tissues (thorax vs. abdomen/fat body/Malpighian tube/head: $p < 0.05$). Abdomen expression followed, but was significantly lower than that in the thorax (abdomen vs. thorax: $p < 0.05$). *EiSD* expression in the fat body and Malpighian tubules was intermediate, while the head showed the lowest expression, with significant differences observed when compared to other tissues (head vs. thorax/abdomen/fat body/Malpighian tubes: $p < 0.05$) (Fig. 11).

The relative expression levels of *EiSD* at five different temperature points (12, 18, 24, 30, and 36 °C) in 5th instar larvae showed significant changes. *EiSD* expression reached its peak at 30 °C and was second highest at 24 °C, with notable increases compared to 12, 18, and 36 °C (30°C vs. 12/18/36 °C: $p < 0.05$ and 24°C vs. 12/18/36 °C: $p < 0.05$). At 12, 18, and 36°C, the expression levels of the *EiSD* gene were relatively low, with no significant differences detected among these temperatures (Fig. 12).

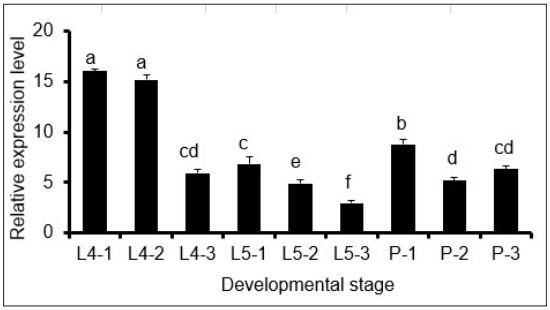

Figure 10. Expression of *EiSD* across developmental stages (4th instar larvae, 5th instar larvae, pupae) of *E. impressicornis*.

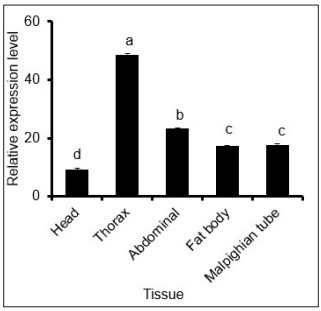

Figure 11. Expression of *EiSD* in different tissues of *E. impressicornis*.

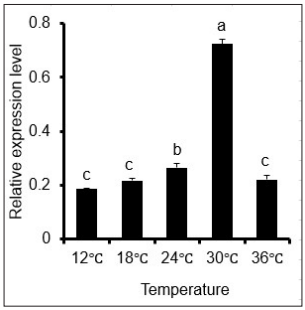

Figure 12 Expression of *EiSD* in 5th instar larvae of *E. impressicornis* under varying temperatures.

DISCUSSION

Sorbitol is metabolized into glycogen via the enzyme sorbitol dehydrogenase, which supplies energy for the diapause period in insects (Zhou, Yuan, Li, Liang, & Li, 2020; Zhao, Wang, Liu, & Torson, 2022). In the present study, we cloned the full-length cDNA sequence of the sorbitol dehydrogenase gene (*EiSD*) from *E. impressicornis*. Structural analysis revealed that the *EiSD* protein exhibits a typical transmembrane domain and displayed hydrophilic characteristics with an average hydrophilicity score of -0.003. It harbored a conserved domain, sorbitol_DH, which is a hallmark of sorbitol dehydrogenase genes (Rubio et al., 2011). The protein also contains three potential

N-glycosylation sites and four phosphorylation sites, which are likely to be instrumental in the functional regulation of the protein (Wang, Wu, & Wang, 2006; Jagannadham, Kameshwari, Gayathri, & Nagaraj, 2018).

Notably, the subcellular localization prediction indicates that the *EiSD* protein is predominantly found in the mitochondria (34.8%) and cytoplasm (30.4%). Combined with its high stability (half-life of 30 h) and moderate instability coefficient (28.72), these characteristics suggest that it may play a significant role in energy metabolism and cellular signal transduction (Zhou et al., 2023).The secondary structure analysis of *EiSD* disclosed that it comprises 62.64% random coil, pointing to its high degree of structural flexibility (Fredslund et al., 2016). The tertiary structure modeling of *EiSD* showed that the protein shares 71.07% amino acid sequence identity with *C. ferrugineus*, and it has a global model quality estimate of 0.97, which affirms its evolutionary conservation. Phylogenetic analysis positioned *EiSD* within a distinct clade with the SD from *T. castaneum*, separate from other Coleoptera SD sequences. SD sequences from various insects —Coleoptera, Diptera, Hymenoptera, and Hemiptera are clustered in accordance with their taxonomic affiliations, those from closely related species positioned near each other, forming distinct clusters on the phylogenetic tree. This finding indicated that SD sequences were highly conserved, and supported the classification of insects into their traditional taxonomic groups (Zhou et al., 2023).

The analysis of developmental stage expression revealed that the expression level of *EiSD* in 5th instar larvae was significantly lower compared with that in 4th instar larvae and pupae, with the lowest expression occurring at 72h during the 5th instar larval stage. This expression pattern indicated that sorbitol metabolism may serve as a crucial energy source during the diapause stage (the 5th instar larval stage) of the flat-horned blister beetle (Liu et al., 2016). The expression analysis of different tissues in the 5th instar larvae indicated that the expression level of *EiSD* is highest in the thoracic tissue, which is consistent with the thorax being the locomotor center of insects that demands substantial energy supply (Sau, Dhillon, & Tanwar, 2024). The temperature response experiment on 5th instar larvae demonstrated that *EiSD* expression peak at 30 °C, while it significantly decreased at temperatures of 12, 18, 24, and 36 °C, showing a trend of decline as temperatures move away from the optimal. This pattern was reminiscent of the temperature-dependent sorbitol synthesis observed in *Epiblema scudderiana* (Clemens) larvae, further supporting the notion that temperature was a key environmental factor regulating *EiSD* expression (Zhou et al., 2023). Consequently, the diminished expression of *EiSD* could result in the accumulation of sorbitol, other sugar alcohols, and glycerol, thus enhancing the insect's resilience under stress conditions (Kojic et al., 2018; Zhou, Yuan, Li, Liang, & Li, 2020; Zhou et al., 2023). The expression pattern of the sorbitol dehydrogenase gene was closely associated with developmental stages, distinct tissues, and environmental temperature, reflecting its critical role in insect adaptation to temperature variations (Wang et al., 2013; Pita, Rico-Porras, Lorite, & Mora, 2025). Nevertheless, the mechanisms by which *EiSD* in 5th instar larvae of *E. impressicornis* mediates resistance to environmental-stress resistance and sustains diapause-overwintering remain to be further elucidated using RNA interference (RNAi) or gene-editing approaches.

This study has successfully cloned the sorbitol dehydrogenase gene (*EiSD*) from *E. impressicornis*. The protein encoded by this gene features characteristic transmembrane domains and multiple sites for post-translational modification. Subcellular localization prediction indicated that it is primarily situated in the mitochondria and cytoplasm. *EiSD* demonstrates a high degree of conservation across Coleoptera insects. During the 5th instar larval stage, *EiSD* expression is low, with the highest levels observed in the thorax. Additionally, its expression is reduced under both low-temperature (12 °C) and high-temperature (36 °C) conditions. It is postulated that *EiSD* may contribute to the ability of *E. impressicornis* to cope with the stress of low winter temperatures and extreme high temperatures. The results of this study enhance the available research information on the *EiSD* gene. While RT-qPCR suggests *EiSD* involvement in stress adaptation, functional studies (e.g., RNA interference) are needed to confirm its role in sorbitol metabolism. Future studies will employ RNA interference (RNAi) or gene-editing techniques to perform targeted functional analyses of the *SD* protein. This approach will facilitate a more precise understanding of the mechanisms underlying the *SD* protein's functions within the organisms.

ACKNOWLEDGMENTS

This research was funded by the Guizhou Province Science and Technology Basic Project [QKHJC-ZK (2023) 018], and the Science-Technology Program of Guizhou Province (ZSYS 2025024). The authors declare that they have no conflicts of interest related to this work.

REFERENCES

Chen, Y.S. & Tu, X.Y. (2013). Research progress on diapause and feeding technique of Meloidae insects and its utilization in bio-control. *China Plant Protection*, 33(05), 16-19+24.

Coloe, J. & Morrell, D.S. (2009). Cantharidin use among pediatric dermatologists in the treatment of *Molluscum Contagiosum*. *Pediatric Dermatology*, 26(4), 405-408.

Dai, X.Y., Wang, Y., Liu, Y., Wang, R.J., Su, L., Yin, Z.J., Zhao, S., Chen, H., Zheng, L., & Dong, X.L. (2024). Molecular correlates of diapause in *Aphidoletes aphidimyza*. *Insects*, 15(5), 299.

Deng, Y.Y., Zhang, W., Li, N.P., Lei, X.P., Gong, X.Y., Zhang, D.M., Wang, L., & Ye, W.C. (2017). Cantharidin derivatives from the medicinal insect *Mylabris phalerata*. *Tetrahedron*, 73(40), 5932-5939.

Duan, Z.Y., Qu, Y.N., Tang, R., Sheng, M.Y., Wang, L.L., Li, J., Zheng, S., & Guo, L.Y. (2025). Case report: persistent toxic reactions in a toddler with a negative blood cantharidin toxicology test. *Frontiers in Pediatrics*, 27(13), 1546669.

Fredslund, F., Otten, H., Gemperlein, S., Poulsen, J.C.N., Carius, Y.,Kohring, G.W., & Lo Leggio, L. (2016). Structural characterization of the thermostable *Bradyrhizobium japonicum* D-sorbitol dehydrogenase. *Acta Crystallographica Section F-Structural Biology Communications*, 72(11), 846-852.

Jagannadham, M.V., Kameshwari, D.B., Gayathri, P., & Nagaraj, R. (2018). Detection of peptides with intact phosphate groups using MALDI TOF/TOF and comparison with the ESI-MS/MS. *European Journal of Mass Spectrometry*, 24(2), 231-242.

Jakovac-Strajn, B., Brozic, D., Tavcar-Kalcher, G., Babic, J., Trilar, T., & Vengust, M. (2021). Entomological surveillance and cantharidin concentrations in *Mylabris variabilis* and *Epicauta rufidorsum* blister beetles in Slovenia. *Animals*, 11(1), 220.

Jiang, C.Y., Wu, Q., Yang, N.W., Huang C., Liu W.X., Qian, W.Q., & Wan, F.H. (2021). The molecular regulation of diapause induction in insects. *Journal of Applied Entomology*, 58(1), 1-13.

Kojic, D., Popovic, Z.D., Orcic, D., Purac, J., Orcic, S., Vukasinovic, E.L ., Nikolic, T.V., & Blagojevic, D.P. (2018). The influence of low temperature and diapause phase on sugar and polyol content in the European corn borer *Ostrinia nubilalis* (Hbn.). *Journal of Insect Physiology*, 109, 107-113.

Landau, S. & Everitt, B. (2004). A handbook of statistical analyses using SPSS. Boca Raton, BR: Chapman & Hall/CRC.

Liu, Y.Y., Zhou, Z.C., & Chen, X.S. (2020). Characterization of the complete mitochondrial genome of *Epicauta impressicornis* (Coleoptera: Meloidae) and its phylogenetic implications for the infraorder Cucujiformia. *Journal of Insect Science*, 20(2), 1-10.

Liu, Y.Y., Li, G.Y., Yang, L., Chi, H., & Chen, X.S. (2018). Demography and mass rearing of the medicinal blister beetle *Epicauta impressicornis* (Pic) (Coleoptera: Meloidae) at different temperatures. *Journal of Economic Entomology*, 111(5), 2364-2374.

Liu, Y.Y., Zhou, Z.C., & Chen, X.S. (2024). The morphology, effects of temperature and photoperiod on pseudopupal diapause and low temperature storage of *Epicauta impressicornis* (Coleoptera: Meloidae). *Journal of the Entomological Research Society*, 26(3), 441-453.

Livak, K.J. & Schmittgen, T.D. (2001). Analysis of relative gene expression data using real-time quantitative PCR and the $2^{-\Delta\Delta C(T)}$ Method. *Methods*, 25(4), 402-408.

Marks, C.P. (2020). Embryonic temperature shifts increase adult size in *Drosophila melanogaster*. *The FASEB Journal*, 34(S1), 1.

Milagre, C.D.F. & Milagre, H.M.S. (2022). Alcohol dehydrogenase-catalyzed oxidation. *Current Opinion in Green and Sustainable Chemistry*, 38, 100694.

Mohammadzadeh, M., Borzoui, E., & Izadi, H. (2017). Physiological and biochemical differences in diapausing and nondiapausing larvae of *Eurytoma plotnikovi* (Hymenoptera: Eurytomidae). *Environmental Entomology*, 46(6), 1424-1431.

Pita, S., Rico-Porras, J.M., Lorite, P., & Mora, P. (2025). Genome assemblies and other genomic tools for understanding insect adaptation. *Current Opinion in Insect Science*, 68, 101334.

Rubio, R.O., Suzuki, A., Mitsumasu, K., Homma, T., Niimi, T., Yamashita, O., & Yaginuma, T. (2011). Cloning of cDNAs encoding sorbitol dehydrogenase-2a and b, enzymatic characterization, and up-regulated expression of the genes in *Bombyx mori* diapause eggs exposed to 5°C. *Insect Biochemistry & Molecular Biology*, 41(6), 378-387.

Sau, A.K., Dhillon, M.K., & Tanwar, A.K. (2024). Diapause-induced shift in the content of major carbohydrates in *Chilo partellus* (Swinhoe). *Journal of Experimental Zoology Part a-Ecological and Integrative Physiology*, 341(2), 193-202.

Tang, W.C., Pan, Y., Zhu, C., Lou, D.D., Peng, F., Shi, Q., & Xiao, Y.Y. (2024). DDIT4/mTOR signaling pathway mediates cantharidin-induced hepatotoxicity and cellular damage. *Frontiers in Pharmacology*, 5(15), 1480512.

Wang, H.L., Wu, J.X., & Wang, B. L. (2006). Changes of trehalase and sorbitol dehydrogenase activity lin the wheat midge, *Sitodiplosis mosellana*(Gehin) during mature and diapause stage. *Journal of Northwest A&F University (Natural Science Edition)*, 34(8), 139-142.

Wang, M.Q. & Li, Z.Z. (2004). The research advance of insect diapause. *Journal of Nanjing Forestry University (Natural Sciences Edition)*, 28(1), 71-76.

Wang, T., Hou, M., Zhao, N., Chen, Y.F., Lv, Y., Li, Z.R., Zhang, R., Zou, X.Y., & Hou, L. (2013). Cloning and expression of the sorbitol dehydrogenase gene during embryonic development and temperature stress in *Artemia sinica*. *Gene*, 521(2), 296-302.

Xie, Z.F., Xu, L.C., Zhao, J., Li, N., Qin, D.Q., Xiao, C., Lu, Y.Y., & Guo, Z.J. (2023). Rapid cold hardening and cold acclimation promote cold tolerance of oriental fruit fly, *Bactrocera dorsalis* (Hendel) by physiological substances transformation and cryoprotectants accumulation. *Bulletin of Entomological Research*, 113(4), 574-586.

Liu, Y., Gao, H., Xue, J.L., Wu J.X., Cheng, W.N., & Ke-Yan, Z.S. (2016). Changes in sorbitol content and the expression level off sorbitol dehydrogenase gene in *Sitodiplosis mosellana* (Diptera: Cecidomyiidae) larvae at different diapause stages. *Acta Entomologica Sinica*, 59(02), 119-126.

Yang, T.F., Yu, R.Z., Cheng, C., Huo, J., Gong, Z.Y., Cao, H.B., Hu, Y., Dai, B.L., & Zhang, Y.M. (2023). Cantharidin induces apoptosis of human triple negative breast cancer cells through mir-607-mediated downregulation of *EGFR*. *Journal of Translational Medicine*, 21(1), 597.

Zhao, L.Q., Wang, X.M., Liu, Z., & Torson, A.S. (2022). Energy consumption and cold hardiness of diapausing fall webworm pupae. *Insects*, 13(9), 853.

Zhou, H.J., Su, M.S., Du, J.H., Zhang, X.A., Li, X.W., Zhang, M.H., Hu, Y., Huan, C., & Ye, Z.W. (2023). Crucial roles of sorbitol metabolism and energy status in the chilling tolerance of yellow peach. *Plant Physiology and Biochemistry*, 204, 108092.

Zhou, Z.X., Yuan, J.J., Li, S.X., Liang, L., & Li, C.R. (2020). Activity of trehalase and sorbitol dehydrogenase of the Chinese citrus fruit fly, *Bactrocera minax* (Enderlein) during diapause period. *Plant Protection*, 46(4), 144-48.

Zou, M.S., Xu, Y.L., Lin, P., Zhou, L.L., & Xia, X.H. (2023). Use of different ligand modification liposomes to evaluate the anti-liver tumor activity of cantharidin. *Journal of Liposome Research*, 33(3), 283-299.